Biocatalysis and Agricultural Biotechnology 18 (2019) 100894

Contents lists available at ScienceDirect

Biocatalysis and Agricultural Biotechnology

journal homepage: www.elsevier.com/locate/bab

Euphorbia heterophylla (L.) mediated fabrication of ZnO NPs: Characterization and evaluation of antibacterial and anticancer properties

K. Lingaraju[a], H. Raja Naika[a,*], H. Nagabhushana[b], G. Nagaraju[c]

[a] Department of Studies and Research in Biotechnology, Tumkur University, Tumakuru 572103, India
[b] Prof. C.N.R. Rao Centre for Advanced Material Science, Tumkur University, Tumakuru 572103, India
[c] Department of Chemistry, Siddaganga Institute of Technology, Tumakuru 572103, India

ARTICLE INFO

Keywords:
Green synthesis
E.heterophylla (L.)
ZnO NPs
Antibacterial activity
Cytotoxicity

ABSTRACT

Euphorbia heterophylla leaves extract mediated synthesis of multifunctional Zinc oxide nanoparticles (ZnO NPs) by green chemistry approaches. The prepared product was well characterized using various analytical tools namely X-ray diffraction (XRD), Ultra Violet-Diffused reflectance spectroscopy (UV-DRS), Fourier transform infrared spectroscopy (FT-IR), Raman spectroscopy, Scanning electron microscopy (SEM), Energy dispersive X-ray analysis (EDAX) and Transmission electron microscopy (TEM) etc. The XRD pattern of ZnO NPs showed hexagonal phase with wurtzite structure. The UV-DR Spectrum reveled that characteristic peak at 370 nm and its energy band gap was found to be ~3.15 eV indicating the formation of ZnO NPs. The FT-IR spectrum results showed the presence of functional groups. The Raman spectrum showed the presence of phonon modes of vibrations in ZnO NPs. The morphological analysis of ZnO NPs exhibit hexagonal, conical and pyramidal nature with mean particle size of ~40 nm which is in close agreement with XRD pattern. ZnO NPs shows significant antibacterial activity against pathogenic bacterial strains both Gram positive and Gram negative bacteria by agar well diffusion method. Furthermore, the cytotoxicity of ZnO NPs was evaluated against cancer cell lines such as lung (A549) and hepatocellular carcinoma (HepG2) cell lines. Therefore, the study reveals that, the *E. heterophylla* is an effective reducing agent for the formation of ZnO NPs with significant antibacterial and cytotoxicity properties.

1. Introduction

In recent years, metal oxide nanoparticles have gained significant attention in scientific research due to their unique properties in physical, chemical and biological sciences (Mirzaei and Darroudi, 2014). Among them, ZnO NPs are well known segment of materials due to their unique properties in different applications (Zhang et al., 2018; Xiang et al., 2017a, 2017b). Zinc oxide (ZnO) is a wide band gap n-type semiconducting material which exhibits band gap ~3.37 eV with large exciting binding energy (Patel et al., 2015). The morphological analysis of ZnO has been fascinated by numerous superstructures namely bullets, flower, plates, prismatic tip etc. (Madan et al., 2016; Udayabhanu et al., 2016). Therefore, the design, synthesis and morphological features of ZnO NPs exhibiting unique properties is of great interest in the field of research.

The various methods are design for the synthesis of ZnO nanoparticles such as laser ablation, electrochemical depositions, sol-gel method, chemical vapor deposition, thermal decomposition, ultrasound, co-precipitation, electrophoretic deposition etc. (Zhao et al., 2011; Manjunath et al., 2014; Streckovaa et al., 2012; Li et al., 2008). These methods are expensive, have tedious protocols, needs sophisticated equipment, and runs in rigorous experimental conditions. However, some of the researchers interested towards green synthesis of metal oxide nanoparticles with simple, cost-effective, biocompatible and eco-friendly routes (Bheemanagouda et al., 2016; Vidya et al., 2013). The biological process involves the green synthesis of nanoparticles using plants materials (Root, stem, leaves, flower, fruit and seeds) and microorganisms like bacteria, fungi, algae, yeast etc. (Rajiv et al., 2013; Iravani, 2013; Elumalai et al., 2015; Ramesh et al., 2015; Pavithra et al., 2017). ZnO NPs prepared with green route, exhibits various nanostructures which influence the diverse properties (Sangani et al., 2015; Hameed et al., 2016; Jain et al., 2014; Namvar et al., 2016; Al-mi et al., 2018).

Euphorbia heterophylla (Linn.) is a branched shrub belongs to the family *Euphorbiaceae*, widely distributed in South and Southeast Asian countries and has become a weed in India and Thailand. *Euphorbia*

* Corresponding author.
E-mail address: rajanaika@tumkuruniversity.ac.in (H.R. Naika).

https://doi.org/10.1016/j.bcab.2018.10.011
Received 20 September 2018; Accepted 15 October 2018
Available online 24 October 2018
1878-8181/

heterophylla (Linn.) has been used as anti-gonorrhea and also for the treatment of common ailment in traditional medicine. Furthermore, it also can be used to treat constipation, bronchitis, asthma, laxative and as lactogenic agent (Falodun and Agbakwuru, 2004). The plant material of *E. heterophylla* was extensively used for pharmacological studies such as antimicrobial, antioxidant, anti-inflammatory, anticancer, anti-diabetic and wound healing activity (Uduak et al., 2010; Kesavan et al., 2014; Falodun et al., 2006; Meenakshi Sundaram et al., 2010; Omale and Emmanuel, 2010).

Herein, we report the synthesis of ZnO NPs for the first-time using *E. heterophylla* as a reducing/capping agent or fuel by combustion method (Suresh et al., 2015; Nagabhushana et al., 2016). The obtained product was well characterized using various analytical techniques such as X-ray diffraction (XRD), Ultra violet-diffuse reflectance spectroscopy (UV-DRS), Fourier transform infrared spectroscopy (FT-IR), Raman spectroscopy, Scanning electron microscopy (SEM), Transmission electron microscopy (TEM) and Energy dispersive x-ray analysis (EDAX). The antibacterial activity of green synthesis of *E.heterophylla* assisted zinc oxide nanoparticles (E-ZnO NPs) was screened against pathogenic bacterial strains both Gram positive and Gram negative bacteria by agar well diffusion method. In addition to this, the cytotoxicity of ZnO NPs was evaluated against human cancer cell lines such as lung (A549) and hepatocellular carcinoma (HepG2) cell lines.

2. Materials and methods

2.1. Materials

All the chemicals used were analytical grade. Doubled distilled water was used for the preparation of all reagent's solutions. The chemicals were purchased from Sigma Aldrich, SD-Fine and Himedia laboratories Pvt. Ltd, India.

2.2. Collection, identification and preparation of extract from plant

The *Euphorbia heterophylla* (L.) plant was collected from Tumkur University campus, Tumakuru, Karnataka, India. The plant was identified and authenticated by Prof. V. Krishna, Department of Biotechnology and Bioinformatics, Kuvempu University, Shimoga, Karnataka, India. Then after, the leaves of *E.heterophylla* was washed with running tap water and followed by doubled distilled water to remove the dust particles and shaded dried at room temperature. after dried, the leaves were pulverized with electric blender and then extract was prepared with doubled distilled water using Soxhlet apparatus (Raja Naika and Krishna, 2006) by maintaining the temperature at 60–70 °C for 72 h. After extraction process, the extract was dried and stored at 4 °C until further use.

2.3. Synthesis of zinc oxide nanoparticles (ZnO NPs)

Synthesis of ZnO NPs by ecofriendly green chemistry approaches (Combustion route) using *E.heterophylla* leaves extract as a reducing agent/capping agent/fuel. In a typical synthesis process, ZnO NPs was prepared in the ratio of 1:9 the *E.heterophylla* leaves extract and zinc nitrate hexahydrate (oxidizer) were dissolved in doubled distilled water in a beaker and stirred for 10 min to get the homogenous solution. The solution was kept in a pre-heated muffle furnace at 400 ± 5 °C. Smoldering type of reaction was observed which is completed in less than 5 min. The product was calcined at 500 °C for 3 h to remove the impurities and formation of ZnO NPs. The main mechanism of the synthesis of nanoparticles is, the biomolecules present in the leaf extract form a complex with the oxidizer, which scaffolds the reducing/capping agent to react with the metal ions. Therefore, leaf extract acts as scaffolds (direct the formation of nanoparticles), stabilizing agent (adheres onto the surface of the nanoparticles) and also as a protective layer which controls the particle size (Vijayakumar et al., 2016).

2.4. Characterization

The green synthesized nanoparticles were subjected to X-ray diffraction employing Shimadzu X-ray diffractometer (PXRD-7000) with monochromatized CuKα (1.541 Å) radiation with nickel filter for determining the phase purity and crystallinity of the sample. The optical properties of nanoparticles were characterized by using Perkin Elmer Lambda-35 Spectrophotometer. The Fourier transform infrared spectroscopic measurements of nanoparticles were performed using Perkin Elmer Spectrum BX FT-IR system. Raman studies of nanoparticles were carried out using HORIBA Lab Ram HR800 spectrometer with recorded at several different spots in back scattering geometry using 514.5 nm Ar^+ laser. The surface morphology of nanoparticles was analyzed using scanning electron microscopy (SEM, Hitachi 3000) and transmission electron microscopy (TEM) (JEOL TEM 3010) fitted with a Gatan CCD camera operating at an accelerating Voltage of 300 kV. The Energy dispersive X-ray Analysis (EDAX) used for compositional analysis of the nanoparticles.

2.5. Antibacterial activity

Antibacterial activity of ZnO NPs were screened against four pathogenic bacterial stains both Gram positive bacteria [*Staphylococcus aureus* (NCIM-5022)] and Gram negative bacterial [*Escherichia coli* (NCIM-5051), *Pseudomonas desmolyticum* (NCIM-2028) and *Klebsiella aerogenes* (NCIM-2098)] strains (Purchased from NCL Pune, India) by Agar well diffusion method (Sawai, 2003; Rizwan et al., 2010). Nutrient agar (NA) media (Hi media laboratories Pvt. ltd, Mumbai, India) was used for bactericidal activity of E-ZnO NPs in-vitro condition. Nutrient agar plates were prepared by using 37.0 g of nutrient agar media (NA) (composition of NA contains peptone 10 g; beef extract 10 g; sodium chloride 5 g; agar 12 g; pH adjusted to 7.3 ± 0.1) was dissolved in 1000 mL of distilled water, and then subject to the sterilization by autoclave at 15 lbs pressure (121 °C) for 15–20 min. After sterilization, NA medium was poured into sterile petri-dishes and allowed to solidify, then, 100 µl of 24 h mature broth culture of individual pathogenic bacterial strains in nutrient broth spreaded all over the surface of agar plates using sterilized L-shaped glass rod. Thereafter, using the sterile steel cork borer 06 mm, wells were made in each petriplate under aseptic condition. Various concentrations of ZnO NPs (250, 500, 750, 1000 µg/µl) were used to assess the dose dependent activity of the product. E-ZnO NPs was dispersed in 10% DMSO solution using ultrasonicator and then sterilized micropipettes were used for the addition of dispersed ZnO NPs into the wells. Similarly, the ciprofloxacin (positive control) as a standard antibiotic used for bacterial strains. After addition of sample in NA, plates were incubated at 37 °C for 24 h using incubator. After incubation, to observe the bactericidal activity of standard drug containing ciprofloxacin, control and ZnO NPs showing the inhibition zone of each well and then measured values were noted using geometrical vernier callipers in mm. The bactericidal activity was carried out in triplicates with each compound and then the average values were calculated for determining the bactericidal activity.

2.6. Anticancer activity

The cytotoxicity of E-ZnO NPs was evaluated by using MTT 3-(4,5-dimethylthiazol-2-yl)-2,5-diphenyltetrazolium bromide assay protocol (Dhaneswar et al., 2013; Kavitha et al., 2016). The cancerous cell lines such as human lung cancer cells (A549) and human hepatocarcinoma cell (HepG2) were procured from National Centre for Cell Science, Pune, India. The cell lines were grown in Dulbecco's Modified Eagle's Medium (DMEM) with supplemented fetal bovine serum with antibiotics and then incubated at 37 °C in the presence of humidified atmosphere of 5% CO_2 and cell lines were grown for 24 h before the experiment. The cancer cell lines were seeded in 96 well plates at a density 25 × 10^3 cells/well and incubated for 24 h. After incubation,

A549 and HepG2 cells were treated with various concentrations of ZnO NPs (25, 50, 100, 200 and 400 µg/µl). After treatment, the 96-well plates were incubated for 24 h. Thereafter, the treated cells were incubated with 10% of MTT DMEM for 3 h. The culture medium was extracted, and then added 100 µl DMSO to each well. Cell viability was determined by measuring the absorbance at 570 nm (Microplate reader-spectro star nano, BMG Labtech, Germany). All the experiments were carried out in triplicates and then the values are calculated with respective percentage of viable cells at different test concentrations with relative untreated cells.

$$\% \text{ of cell viability} = \frac{\text{A570 of treated cell}}{\text{A 570 of controlled cell}} \times 100 \quad (1)$$

Simultaneously the standard antibiotics (Cisplatin used as a positive control) are tested against A549 and HepG2 cell lines. A different concentration of ZnO NPs were have resulted in 50% inhibition of cell growth was calculated as the half maximal inhibitory concentration.

2.7. Statistical analysis

The experimental data was analyzed by mean ± SE subjected to multivariant analysis. Means were separated by Tukey's range tests using eZ ANOVA software.

3. Result and discussion

Presently, the plant mediated synthesis of Nanoparticles is gaining importance due to their simplicity, environmentally friendly and it exhibiting the multifunctional properties of the nanoparticles. Among them, green synthesis of ZnO NPs from *E. heterophylla* [L.] is very simple, inexpensive and ecofriendly nature.

3.1. X-ray diffraction (XRD) analysis

In a Fig. 1. shows the XRD pattern of ZnO NPs from *E. heterophylla*. The characteristics patterns are corresponding to the diffraction patterns of hexagonal wurtzite phase, no other peaks appeared in the XRD pattern. All the diffraction peaks of ZnO NPs are well matched in JCPDS Card no. 36–1451 with lattice parameters are a = 3.24982 Å, c = 5.20661 Å and the space group is *P63mc*. The average crystallite size of ZnO NPs was found to be ˜30 nm which was calculated from the XRD pattern using Debye Scherer's formula (Nagabhushana et al., 2014).

$$D = \frac{k\lambda}{\beta \cos\theta} \quad \text{.....[2]}$$

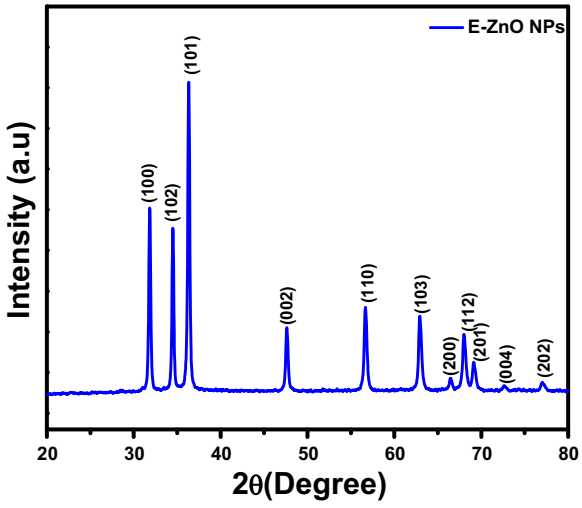

Fig. 1. PXRD pattern of ZnO NPs from *Euphorbia heterophylla* (L.).

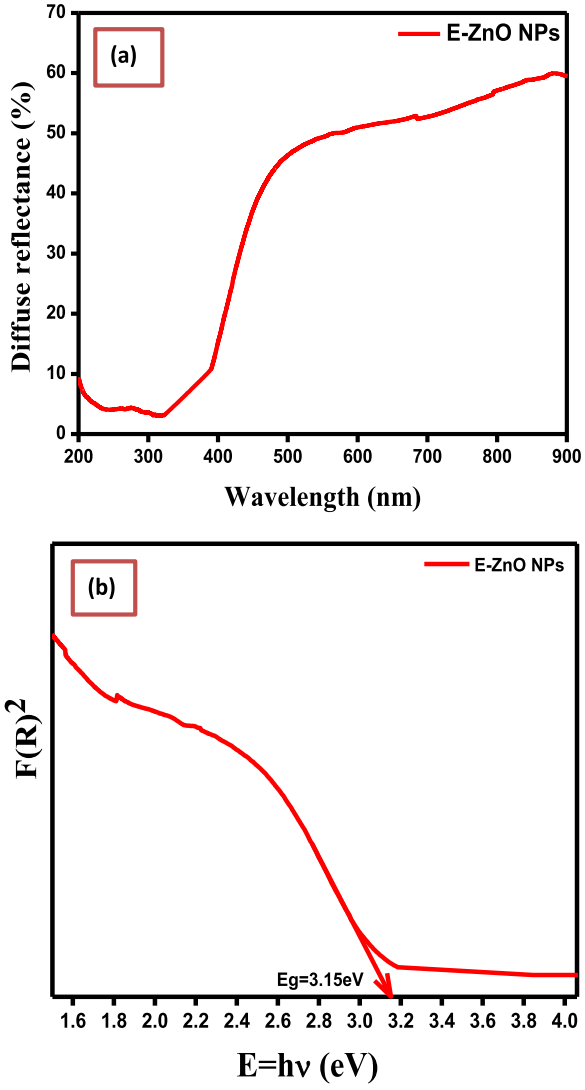

Fig. 2. (a) UV-Diffuse reflectance spectrum (DRS) and (b) Energy band gap (Eg) of ZnO NPs from *E.heterophylla* (L.).

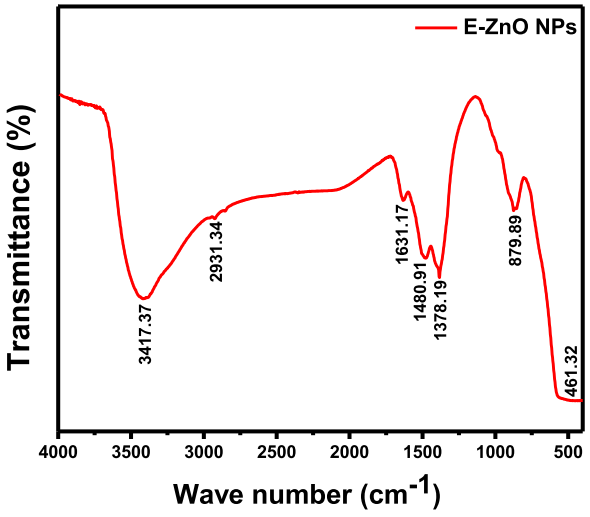

Fig. 3. FT-IR spectrum of ZnO NPs from *E.heterophylla* (L.).

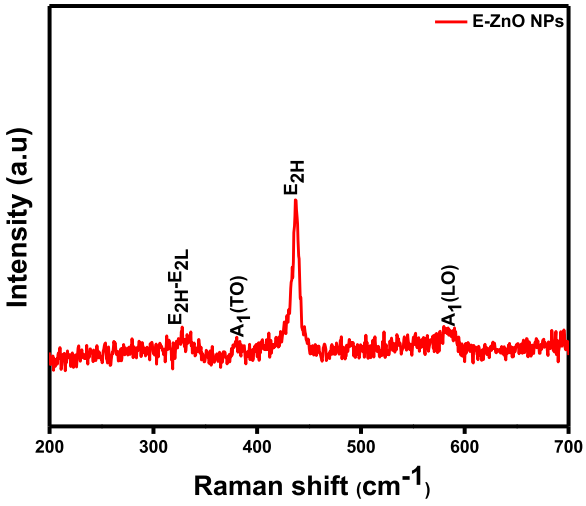

Fig. 4. Raman spectrum of ZnO NPs from *E.heterophylla* (L.).

where 'D' crystallite size of the ZnO NPs, 'k' shape factor (0.9), 'λ' wavelength of X-ray (1.54 Å) Cu Kα radiation, 'θ' is the Bragg angle form 2θ value of intensity peak from XRD pattern and 'β' is the full width half maximum of the diffraction from XRD pattern of ZnO NPs.

3.2. Ultra-Violet diffuse reflectance spectroscopic (UV-DRS) analysis

The UV-DR spectrum of E-ZnO NPs was recorded in between 200 and 900 nm as shown in the Fig. 2. In a Fig. 2(a) show the broad intense reflectance peak at 370 nm. It indicates that, ZnO NPs are transfer of electrons from the valence band to conduction band. The energy band gap of ZnO NPs was calculated by Kubelka-Munk equation (Morales et al., 2007; Kumar et al., 2013) which is based on the transformation of DRS measurements to estimate the values with good accuracy. The energy band gap of ZnO NPs was found to be 3.15 eV as shown in the Fig. 2(b). As a result, ZnO NPs show blue shift with respective to its bulk ZnO which can be attributed to the changes in their surface morphology and size (Vinod Kumar et al., 2010; Mishra et al., 2012).

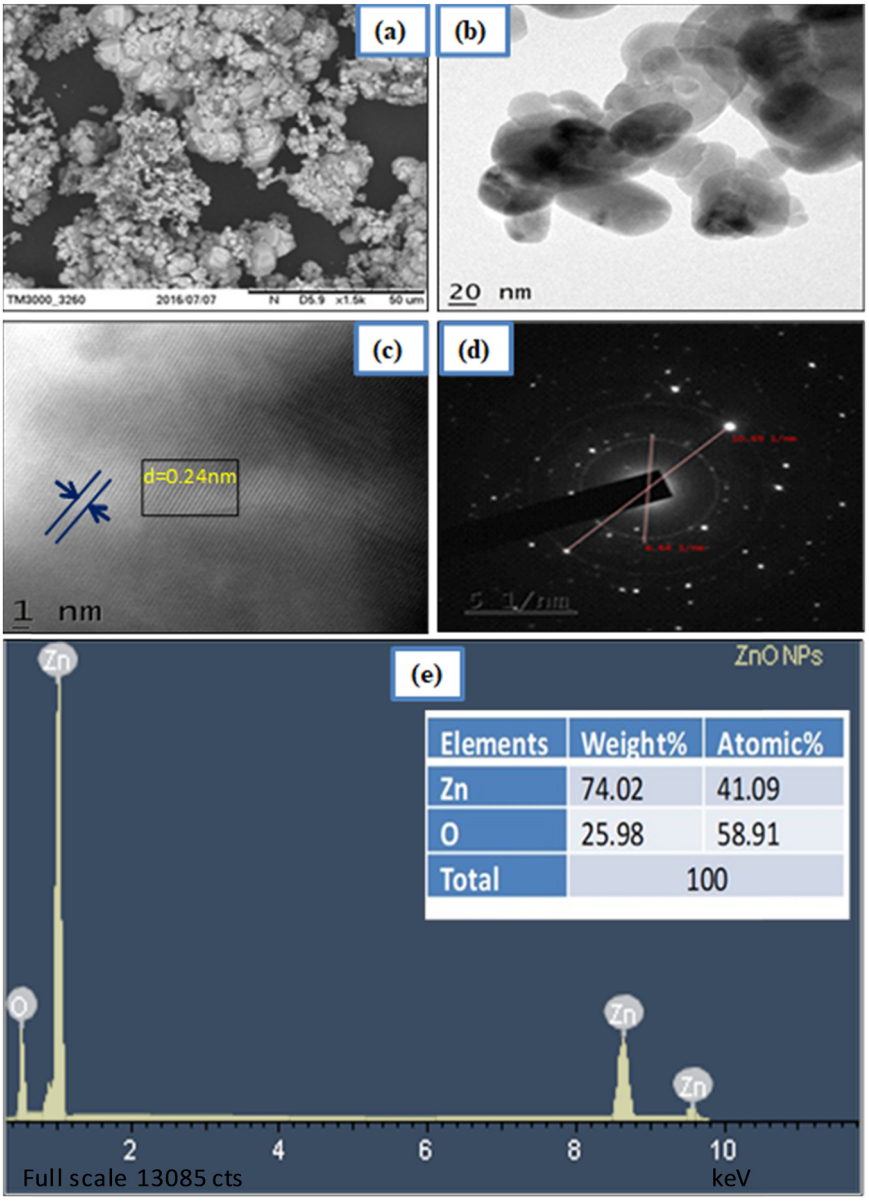

Fig. 5. Morphological analysis of ZnO NPs from *E.heterophylla* (L.) as (a) SEM micrograph (b) TEM image (c) HRTEM (d) SAED pattern (e) EDAX.

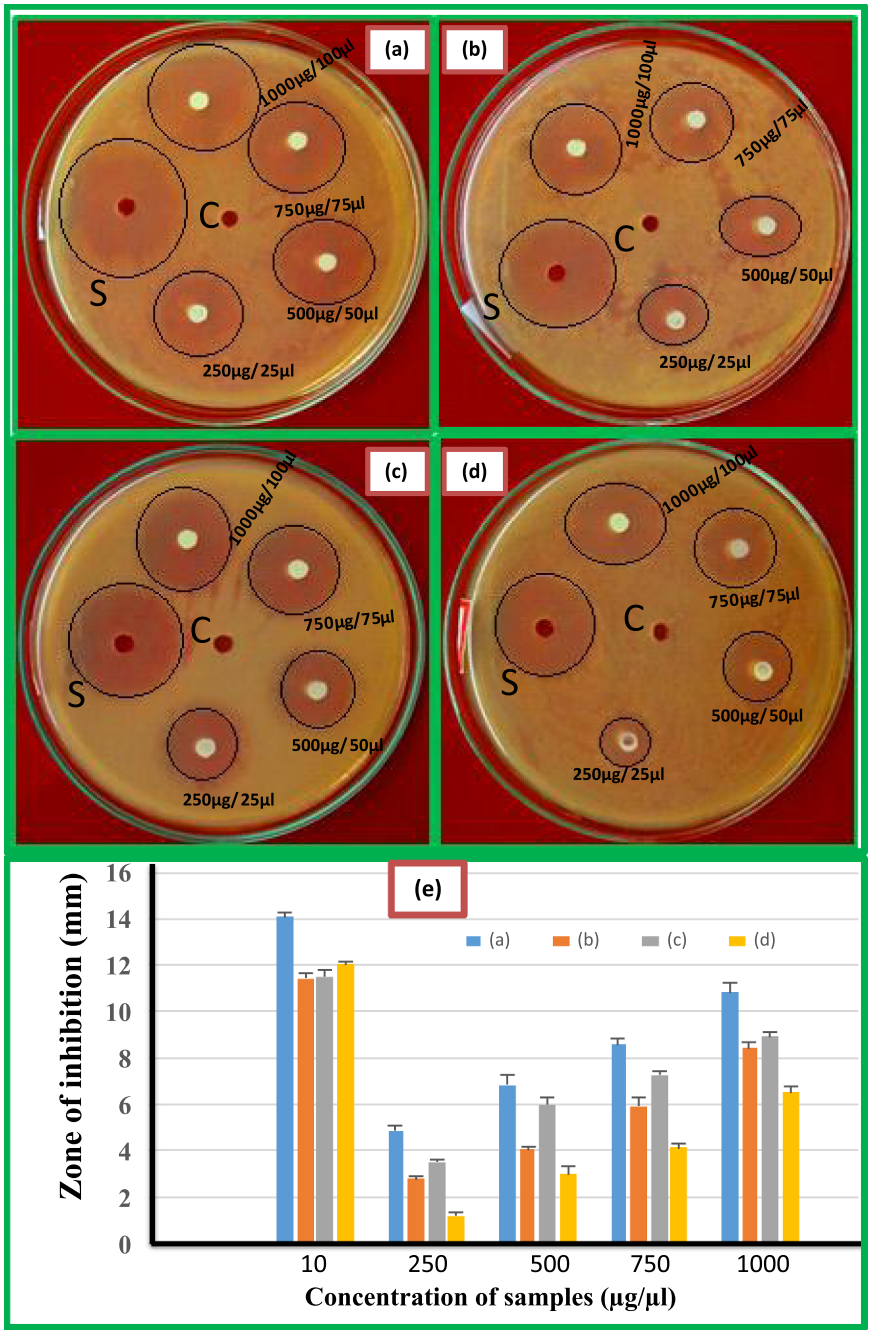

Fig. 6. Antibacterial activity of ZnO NPs from *E. heterophylla* (L.) against bacterial strains such as (a) *S. aureus* (b) *E. coli* (c) *P. desmolyticum* (d) *K. aerogenes* (S = Standard antibiotic; C = Control and different concentration of ZnO NPs 250,500,750 and 1000µg/µl) (e) Graphical representation of antibacterial activity of NPs.

Table 1
Antibacterial activity of E-ZnO NPs against pathogenic bacterial strains.

Treatment		**Bacterial strains**			
Sample	**Concentration (µg/mL)**	*S. aureus* (Mean ± SE)	*E.coli* (Mean ± SE)	*P.desmolyticum* (Mean ± SE)	*K. aerogenes* (Mean ± SE)
Ciprofloxacin	10	14.08 ± 0.22	11.43 ± 0.23	11.50 ± 0.29	12.02 ± 0.13
E-ZnO NPs	250	4.87 ± 0.19	2.77 ± 0.15	3.53 ± 0.09	1.17 ± 0.17
	500	6.83 ± 0.44	4.03 ± 0.15	6.00 ± 0.29	3.00 ± 0.29
	750	8.58 ± 0.22	5.93 ± 0.35	7.27 ± 0.15	4.13 ± 0.19
	1000	10.83 ± 0.44	8.43 ± 0.23	8.92 ± 0.22	6.50 ± 0.29

Values are the Mean ± SE of inhibition zone in mm.

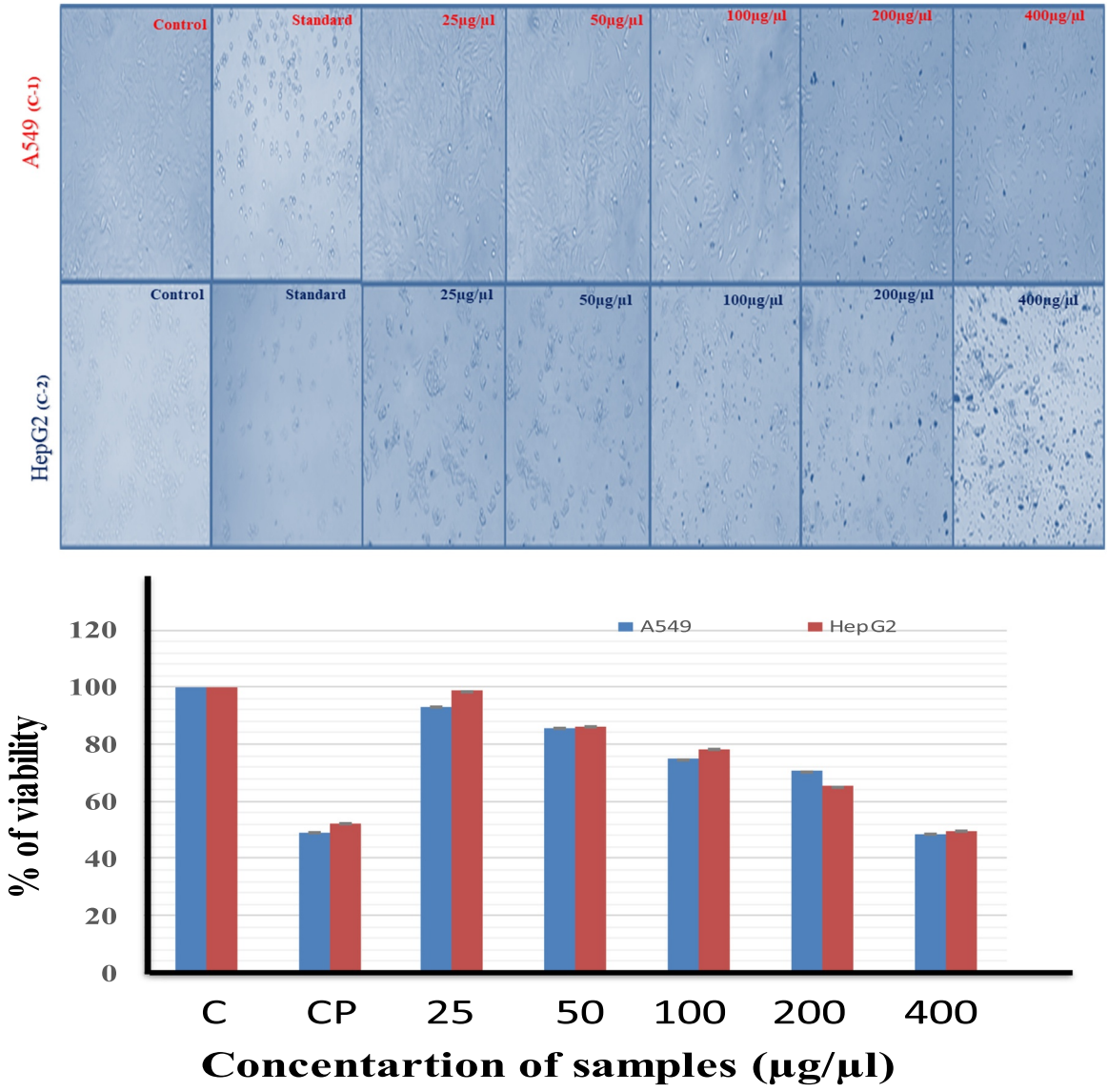

Fig. 7. Cytotoxicity of ZnO NPs from *E.heterophylla* (L.) against A549 (C-1) and HepG2(C-2) cancer cell lines. Control: Cells untreated, Standard: cells treated with drug cisplatin (25 µM): Cells treated with different concentration of ZnO NPs (25, 50, 100, 200, 400 µg/µl) from *E.heterophylla* (L.) and Graphical representation of cytotoxicity of NPs.

Table 2
Cytotoxicity of green synthesis of E-ZnO NPs against cancer cell lines.

Cancerous cell lines	Standard Cisplatin	Concentration of ZnO NPs (µg/µl)						IC_{50} (µg/µl)
	(25 µM)	Control	25	50	100	200	400	383.05
A549	49.09 ± 0.002	100	93.03 ± 0.005	85.64 ± 0.002	74.80 ± 0.003	70.50 ± 0.004	48.66 ± 0.005	
HepG2	52.23 ± 0.005	100	98.58 ± 0.003	86.20 ± 0.004	78.39 ± 0.004	65.31 ± 0.001	49.79 ± 0.001	329.67

3.3. Fourier transform infrared spectroscopy (FTIR) analysis

The FTIR spectrum of E-ZnO NPs was recorded between 4000 and 400 cm^{-1} as shown in the Fig. 3. FTIR spectrum shows a broad band at 3417 cm^{-1} is assigned to O-H stretching mode of water. The peaks observed at 2931, 1631, 1480, 1378 and 880 cm^{-1} are due to symmetrical and asymmetrical stretching and bending vibrations of carboxylic groups. The peak at 461 cm^{-1} is attributed to stretching frequency of the vibrational modes of Zn–O. The results states that, the FTIR spectrum confirms that phenolic compounds in flavonoids are better to bind to the metal ions, indicating that a presence of secondary metabolites may form metal nanoparticles to prevent agglomeration and acts as reducing/stabilizing/capping agent. Its effective role in the presence of biomolecules may perform dual functions such as forming and stabilizing zinc oxide nanoparticles in an aqueous medium (Gnanasangeetha and Sarala, 2014; Sangeetha et al., 2011).

3.4. Raman spectroscopic studies

A vibrational property of E-ZnO NPs was analyzed using Raman spectrum as shown in the Fig. 4. The Raman spectrum exhibits four peaks at 327, 381, 438 and 573 cm^{-1} correspond to E_{2H}- E_{2L}, A_1(TO), E_2H, A_1(LO) fundamental phonon modes of ZnO respectively (Zakhidov et al., 2017). Among them, the phonon modes A_1 and E_1 are polar

which are active in infrared and Raman, while another mode E_2 belongs to non-polar which is active only in Raman spectrum. The second order reaction (E_{2H}-E_{2L}) of vibrational mode at 327 cm^{-1} Raman is active and phonons are inactive with lattice symmetry due to disorder active scattering with attributed in zone boundary phonons. Another phonon A_1 (TO) vibration mode at 3821 cm^{-1} arising due to ZnO polar bond lattice vibrations. The E_{2H} phonon mode shows vibration at 438 cm^{-1} with good crystallite and wurtzite lattices. The A_1(LO) phonon mode shows vibration at 573 cm^{-1} due to defect O_2 vacancy and Zn interstitials in the spectrum of ZnO NPs (Kumar et al., 2009).

3.5. Morphological analysis

Morphological features of E-ZnO NPs is shown in the Fig. 5. The scanning electron microscopy image of ZnO NPs as shown in the Fig. 5(a), the particles are conical, pyramid and triangular in shapes in the presence of plant extract. In a Fig. 5(b), TEM micrograph of ZnO NPs were almost in hexagonal shapes and hexagonal shapes and their sizes are found to be ~40 nm. The obtained particles sizes are in good agreement with the values estimated from XRD analysis. The HR-TEM (High-resolution transmission electron microscopy) images of ZnO NPs show the sample is polycrystalline in nature with inter planar spacing is 0.24 nm which corresponds to (101) plane of hexagonal ZnO is shown in Fig. 5(c). The SAED (Selected area electron diffraction) pattern of ZnO NPs was shown in Fig. 5(d) with 10.69 1/nm and 6.64 1/nm as a scale bar. The EDAX results of ZnO NPs shown in Fig. 5(e) which shows the elemental analysis of zinc, and oxygen atoms with atomic percent (Zn = 41.09. O = 58.91) and weight percent (Zn = 74.02. O = 25.98).

3.6. Antibacterial activity

Antibacterial activity of E-ZnO NPs was screened against various pathogenic bacterial strains (*Staphylococcus aureus*, *Escherichia coli*, *Pseudomonas desmolyticum* and *Klebsiella aerogenes)* by agar well diffusion method. Inhibition zone of E-ZnO NPs with different concentrations (250, 500, 750 and 1000 μg/μl) with respect to the positive control (ciprofloxacin) were shown in the Fig. 6. The antibacterial activity of E-ZnO NPs has shown significant activity in *Staphylococcus aureus* compared to *Escherichia coli*, *Pseudomonas desmolyticum* and *Klebsiella aerogenes* which is shown in Table 1. In a mechanism of antibacterial activity by E-ZnO NPs, Reactive oxygen species (ROS) such as $OH^{\bullet}$ can be generated and recombined to form H_2O_2, which disrupts the cell membrane results in leakage of cytoplasmic contents, can damage DNA which finally leads to cell death. The Zn ions from the ZnO NPs can penetrate into the cell membrane which inhibits the active transport, metabolism of sugar, disrupt metal ion homeostasis and enzyme systems when the concentration reaches a specific level (Lingaraju et al., 2015; Liu et al., 2017; Li et al., 2018; Xie et al., 2017; Li et al., 2017).

3.7. Anticancer activity

The cytotoxicity effects of E-ZnO NPs was evaluated against A549 and HepG2 cells at different concentrations of ZnO (25, 50, 100, 200, 400 μg/μl) by measuring the cellular reduction of tetrazolium dye [MTT 3-(4,5-dimethylthiazol-2-yl)-2,5-diphenyltetrazolium bromide] by its insoluble formazan crystals in-vitro cytotoxicity study (Rajeshkumar et al., 2018). The cytotoxicity of metal oxide nanoparticles against cancer cells has already been reported (Nagajyothi et al., 2014; Fukui et al., 2012). In the present study, E-ZnO NPs with different concentrations were used against i) A549 cancer cell line (C-1) and ii) HepG2-human hepatocarcinoma cell line (C-2), observed a dramatic decrease in cell viability with respect to positive control. The decrease in cell viability with an increase of E-ZnO NPs suggests that accumulation of nanoparticles inside the cells which enhances the cell stress, ultimately leads to cell death. The results clearly showed that there was an enhanced efficacy of E-ZnO NPs against A549 and HepG2 cancer cell lines shows in the Fig. 7. The values in Table 2, shows that highest cytotoxicity effect of E-ZnO NPs were on A549- and HepG2 with IC_{50} value. In a mechanism of cancer cell death, the E-ZnO NPs may induce reactive oxygen species on A549 and HepG2 which penetrates and damages the cellular components, leads to cell death (Song et al., 2010; Wang et al., 2014). The MTT assay yielded concentration-dependent curves in cell lines, indicating the impact of synthesized material in inducing increased cytotoxicity at higher concentrations of nanoparticles.

4. Conclusions

The present work was carried out to investigate the synthesis of multifunctional ZnO NPs by green chemistry route using aqueous leaves extract of *Euphorbia heterophylla* (L.) as a reducing/capping agent/stabilizing agent/fuel. It is a single step for the synthesis of nanoparticles appears to be suitable for large scale production as it is very simple, cost effective, and eco-friendly manner. The as formed product was characterized by using various analytical tools such as XRD, UV-DRS, FT-IR, Raman, SEM, EDX and TEM techniques to study the structural, optical properties and morphological features. Furthermore, the plant derived ZnO NPs exhibits significant biological properties such as antibacterial and anticancer properties. The Antibacterial activity of E-ZnO NPs shows significant inhibitory effect against pathogenic bacterial strains in *S.aureus* when compared to the *E.coli*, *P. desmolyticum* and *K. aerogenes*. In addition to this, E-ZnO NPs shows significant cytotoxic effect on Human Lung Cancer cells (A549) and Human Hepatocarcinoma Cell (HePG2). The results suggest that plant mediated synthesis of ZnO NPs might be of a great value for many biomedical applications.

Acknowledgements

The authors express sincere thanks to Tumkur University, Tumkur, for providing the lab facilities to carry out a part of this work.

References

Al-mi, F.M., Hussain, A., Alsharaeh, E., Ahmed, F., Amir, S., Anwar, M.S., Siddiqui, A.M., Al-Khedhairy, A.A., Koo, B.H., 2018. Green synthesis of zinc oxide nanoparticles using *Alstonia macrophylla* leaf extract and their in-vitro anticancer activity. Sci. Adv. Mater. 10 (3), 349–355.

Bheemanagouda, N., Patil, Tarikere, C., Taranath, 2016. *Limonia acidissima* L. leaf mediated synthesis of zinc oxide nanoparticles: a potent tool against Mycobacterium tuberculosis. Int. J. Mycobacteriol. 5, 197–204.

Dhaneswar, D., ChandraNath, B., Phukon, P., Kalita, A., Kumar Dolui, S., 2013. Synthesis of ZnO nanoparticles and evaluation of antioxidant and cytotoxic activity. Colloid Surf. B: Biointerfaces 11 (1), 556–560.

Elumalai, K., Velmurugan, S., Ravi, S., Kathiravan, V., Ashokkumar, S., 2015. Green synthesis of zinc oxide nanoparticles using *Moringa oleifera* leaf extract and evaluation of its antimicrobial activity. Spectrochim. Acta A Mol. Biomol. Spectrosc. 143, 158–164.

Falodun, A., Agbakwuru, E.O.P., 2004. Phyto-chemical analysis and laxative activity of the leaf extracts of *Euphorbia heterophylla* L. (Euphorbiaceae). Pak. J. Sci. Ind. Res. 47 (5), 345–348.

Falodun, A., Okunrobo, L.O., Uzoamaka, N., 2006. Phytochemical screening and anti-inflammatory evaluation of methanolic and aqueous extracts of *Euphorbia heterophylla* Linn (Euphorbiaceae). Afr. J. Biotechnol. 5 (6), 529.

Fukui, H., Horie, M., Endoh, S., Kato, H., Fujita, K., Nishio, K., Komaba, L.K., Maru, J., Miyauhi, A., Nakamura, A., Kinugasa, S., Yoshida, Y., Hagihara, Y., Iwahashi, H., 2012. Association of zinc ion release and oxidative stress induced by intratracheal instillation of ZnO nanoparticles to rat lung. Chem. Biol. Interact. 198, 29–37.

Gnanasangeetha, D., Sarala, T.D., 2014. Facile and eco-friendly method for the synthesis of zinc oxide nanoparticles using *Azadirachta* and *Emblica*. Int. J. Pharm. Sci. Res. 5 (7), 2866–2873.

Hameed, A.S., Karthikeyan, C., Ahamed, A.P., Thajuddin, N., Alharbi, N.S., Alharbi, S.A., 2016. In vitro antibacterial activity of ZnO and Nd doped ZnO nanoparticles against ESBL producing *Escherichia coli* and *Klebsiella pneumoniae*. Science 6, 24312.

Iravani, S., 2013. Green synthesis of metal nanoparticles using plants. Green. Chem. 13 (10), 2638–2650.

Jain, N., Bhargava, A., Panwar, J., 2014. Enhanced photocatalytic degradation of methylene blue using biologically synthesized “protein-capped” ZnO nanoparticles. Chem. Eng. J. 243, 549–555.

Kavitha, K., Paulpandi, M., Ponraj, T., Murugan, K., Sumathi, S., 2016. Induction of intrinsic apoptotic pathway in human breast cancer (MCF-7) cells through facile

biosynthesized zinc oxide nanorods. Karbala Int. J. Mod. Sci. 2, 46–55.
Kesavan, K., Deepa, A., Shobana, G., Jothi, G., Sridharan, G., 2014. Preliminary phytochemical screening and *invitro* antioxidant potential of *Euphorbia heterophylla* (L.). Int. J. Pharm. Pharm. Sci. 6 (8).
Kumaryadav, H., Gupta, V., Katiyar, R.S., 2009. Structural studies and Raman spectroscopy of forbidden zone boundary phonons in Ni-doped ZnO ceramics. J. Raman Spectrosc. 40, 381.
Kumar, R.G.A., Hata, S., Gopchandran, K.G., 2013. Diethylene glycol mediated synthesis of Gd_2O_3: Eu_3+ nanophosphor and its JuddeOfelt analysis. Ceram. Int. 39, 9125–9136.
Li, F., Hsieh, G.W., Dalal, S., Newton, S., Stott, J.E., 2008. Zinc oxide nanostructures and high electron mobility nanocomposite thin film transistors. IEEE Trans. Electron Dev. 55, 3001–3011.
Li, J., Tan, L., Liu, X., Cui, Z., Yang, X., Yeung, K.W.K., Chu, P.K., Wu, S., 2017. Balancing bacteria−osteoblast competition through selective physical puncture and biofunctionalization of ZnO/polydopamine/arginine-glycine-aspartic acid-cysteine nanorods. ACS Nano 11, 11250–11263.
Li, M., Liu, X., Tan, L., Cui, Z., Yang, X., Li, Z., Zheng, Y., Yeung, K.W.K., Chu, P.K., Wu, S., 2018. Non-invasive rapid bacteria-killing and acceleration of wound healing through photothermal/photodynamic/copper ions synergistic action of a hybrid hydrogel. Biomater. Sci. 6 (8).
Lingaraju, K., RajaNaika, H., Manjunath, K., Basavaraj, R.B., Nagabhushana, H., Nagaraju, G., Suresh, D., 2015. Biogenic synthesis of zinc oxide nanoparticles using *Ruta graveolens* (L.) and their antibacterial and antioxidant activities. Appl. Nanosci. 1, 1–8.
Liu, Z., Zhu, Y., Liu, X., Yeung, K.W.K., Wu, S., 2017. Construction of poly (vinyl alcohol)/poly (lactide −glycolide acid)/vancomycin nanoparticles on titanium for enhancing the surface self-antibacterial activity and cytocompatibility. Colloids Surf. B Biointerfaces 1 (151), 165–177.
Madan, H.R., Sharma, S.C., Udayabhanu, C., Suresh, D., Vidya, Y.S., Nagabhushana, H., Rajanaik, H., Anantharaju, K.S., Prashantha, S.C., Sadananda Maiya, P., 2016. Facile green fabrication of nanostructure ZnO plates, bullets, flower, prismatic tip, closed pine cone: their antibacterial, antioxidant, photoluminescent and photocatalytic properties. Spectrochim. Acta A Mol. Biomol. Spectrosc. 152, 404–416.
Manjunath, K., Ravishankar, T.N., Dhanith Kumar, Priyanka, K.P., Thomas Varghese, Raja Naika, H., Nagabhushana, H., Sharma, S.C., Dupont, J., Ramakrishnappa, T., Nagaraju, G., 2014. Facile combustion synthesis of ZnO nanoparticles using *Cajanus cajan* (L.) and its multidisciplinary applications. Mater. Res. Bull. 7, 325–334.
Meenakshi Sundaram, M., Karthikeyan, K., Sudarsanam, D., Brindha, P., 2010. Antimicrobial and anticancer studies on *Euphorbia heterophylla*. J. Pharm. Res. 3 (9), 2332–2333.
Mirzaei, H., Darroudi, M., 2014. Zinc oxide nanoparticles: biological synthesis and biomedical applications. Ceram. Int. 43, 907–914.
Mishra, S.K., Srivastava, R.K., Prakash, S.G., 2012. ZnO nanoparticles: structural, optical and photoconductivity characteristics. J. Alloy. Compd. 539, 1–6.
Morales, A.E., Mora, E.S., Pal, U., 2007. Use of diffuse reflectance spectroscopy for optical characterization of unsupported nanostructures. Rev. Mex. Fis. S53 (5), 18–22.
Nagabhushana, H., Basavaraj, R.B., Daruka Prasad, B., Sharma, S.C., Premkumar, H.B., Udayabhanu, Vijayakumar, G.R., 2016. Facile EGCG assisted green synthesis of raspberry shaped CdO nanoparticles. J. Alloy. Comp. 669, 232–239.
Nagabhushana, H., Sunitha, D.V., Sharma, S.C., Prasad, B.D., Nagabhushana, B.M., Chakradhar, R.P.S., 2014. Enhanced luminescence by monovalent alkali metal ions in Sr_2SiO_4:Eu3+ nanophosphor prepared by low temperature solution combustion method. J. Alloy. Comp. 575, 192–199.
Nagajyothi, P.C., Sreekanth, T.V.M., Clement O, Tettey, Jun, Y.I., Heung Mook, S., 2014. Characterization antibacterial, antioxidant, and cytotoxic activities of ZnO nanoparticles using *Coptidis Rhizoma*. Bioorg. Med. Chem. Lett. 24 (17), 4298–4303.
Namvar, F., Azizi, S., Rahman, H.S., Mohamad, R., Rasedee, A., Soltani, M., Abdul Rahim, R., 2016. Green synthesis, characterization, and anticancer activity of hyaluronan/zinc oxide Nano composite. Onco Targets Ther. 9, 4549–4559.
Omale, James, Emmanuel, T., 2010. Phytochemical composition, bioactivity and wound healing potential of *Euphorbiaheterophylla* (Euphorbiaceae) leaf extract. Int. J. Pharm. Biomed. Res. 1 (1), 54–63.
Patel, V., Berthold, D., Puranik, P., Gantar, M., 2015. Screening of cyanobacteria and microalgae for their ability to synthesize silver nanoparticles with antibacterial activity. Biotechnol. Rep. 5, 12–119.
Pavithra, N.S., Lingaraju, K., Raghu, G.K., Nagaraju, G., 2017. *Citrus maxima* (Pomelo) juice mediated eco-friendly synthesis of ZnO nanoparticles: applications to photocatalytic, electrochemical sensor and antibacterial activities. Spectrochim. Acta. A: Mol. Biomol. Spectrosc. 185, 11–19.
Raja Naika, H., Krishna, V., 2006. Antimicrobial activity of extracts from the leaves of *Clematis gouriana* Roxb. Int. J. Biomed. Pharm. Sci. 1, 69–72.
Rajeshkumar, S., Venkat Kumar, S., Ramaiah, A., Agarwal, H., Lakshmi, T., Roopan, S.M., 2018. Biosynthesis of zinc oxide nanoparticles using *Mangifera indica* leaves and evaluation of their antioxidant and cytotoxic properties in lung cancer (A549) cells. Enzym. Microb. Technol. 117, 91–95.
Rajiv, P., Rajeshwari, S., Venkatesh, R., 2013. Bio-Fabrication of zinc oxide nanoparticles using leaf extract of *Parthenium hysterophorus* L. and its size-dependent antifungal activity against plant fungal pathogens. Spectrochim. Chim. Acta A Mol. Biomol. Spectrosc. 112, 384–387.
Ramesh, M., Anbuvannan, M., Viruthagiri, G., 2015. Green synthesis of ZnO nanoparticles using *Solanum nigrum* leaf extract and their antibacterial activity. Spectrochim. Acta A Mol. Biomol. Spectrosc. 136, 864–870.
Rizwan, W., Young-Soon, K., Amrita, M., Soon, Y., Hyung-Shik, Sh, 2010. Formation of ZnO micro-flowers prepared via solution process and their antibacterial activity. J. Nanoscale Res. Lett. 5, 1675–1681.
Sangani, M.H., Moghaddam, M.N., Mahdi, M., 2015. Inhibitory effect of zinc oxide nanoparticles on *Pseudomonas aeruginosa* biofilm formation. Nanomed. J. 2 (2015), 121–128.
Sangeetha, G., Rajeshwari, S., Venkatesh, R., 2011. Green synthesis of zinc oxide nanoparticles by *Aloe barbadensis miller* leaf extract: structure and optical properties. Mater. Res. Bull. 46 (12), 2560–2566.
Sawai, J., 2003. Quantitative evaluation of antibacterial activities of metallic oxide powders (ZnO, MgO and CaO) by conduct metric assay. J. Micro. Met. 54, 177–182.
Song, W., Zhang, J., Guo, J., Zhang, J., Ding, F., Li, L., Sun, Z., 2010. Role of the dissolved zinc ion and reactive oxygen species in cytotoxicity of ZnO nanoparticles. Toxicol. Lett. 199, 389–397.
Streckovaa, M., Sopcaka, T., Medvecky, L., Bures, R., Faberovaa, M., 2012. Preparation, chemical and mechanical properties of micro composite materials based on Fe powder and phenol-formaldehyde resin. Chem. Eng. 180, 343–353.
Suresh, D., Nethravathi, P.C., Rajanaika, H., Nagabhushana, H., Sharma, S.C., 2015. Green synthesis of multifunctional zinc oxide (ZnO) nanoparticles using *Cassia fistula* plant extract and their photodegradative, antioxidant and antibacterial activities. Mater. Sci. Semicond. Process. 31, 446–454.
Udayabhanu, Nagaraju, G., Nagabhushana, H., Basavaraj, R.B., Raghu, G.K., Suresh, D., Rajanaika, H., Sharma, S.C., 2016. Green, nonchemical route for the synthesis of ZnO superstructures, evaluation of its applications toward photocatalysis, photoluminescence, and bio sensing. Cryst. Growth Des. 16 (12), 6828–6840.
Uduak, A., Essiett, K., Kola, Ajibesin, 2010. Antimicrobial activities of some euphorbiaceae plants used in the traditional medicine of Akwa Ibom State of Nigeria. Ethnobot. Leaf. 14, 654–664.
Vidya, C., Hiremath, S., Chandraprabha, M.N., Antonyraj, M.A.L., Gopala, I., Jain, A., 2013. Green synthesis of ZnO nanoparticles by *Calotropis gigantea*. Int. J. Curr. Eng. Technol. 1, 118–120.
Vijayakumar, S., Vaseeharan, B., Malaikozhundan, B., Shobiya, M., 2016. *Laurus nobilis* leaf extract mediated green synthesis of ZnO nanoparticles: characterization and biomedical applications. Biomed. Pharm. 84, 1213–1222.
Vinod Kumar, R., Navas, I., Chalana, S.R., Gopichandran, K.G., Ganesan, V., Reji, P., Sudheer, S.K., Mahadevan Pillai, V.P., 2010. Highly conductive and transparent laser ablated nanostructured Al: ZnO thin films. Appl. Surf. Sci. 257, 708–716.
Wang, B., Zhang, Y., Mao, Z., Yu, D., Gao, C., 2014. Toxicity of ZnO nanoparticles to macrophages due to cell uptake and intracellular release of zinc ions. J. Nanosci. Nanotechnol. 14, 5688–5696.
Xiang, Y., Li, J., Liu, X., Cui, Z., Yang, X., Yeung, K.W.K., Pan, H., Wu, S., 2017a. Construction of poly (lactic-co-glycolic acid)/ZnO nanorods/Ag nanoparticles hybrid coating on Ti implants for enhanced antibacterial activity and biocompatibility. Mater. Sci. Eng. C. Mater. Biol. Appl. 79, 629–637.
Xiang, Y., Liu, X., Mao, X., Cui, Z., Yang, X., Yeung, K.W.K., Zheng, Y., Wu, S., 2017b. Infection-prevention on Ti implants by controlled drug release from folic acid/ZnO quantum dots sealed titania nanotubes. Mater. Sci. Eng. C (17), 33350–33357 S0928-4931.
Xie, X., Mao, C., Liu, X., Zhang, Y., Cui, Z., Yang, X., Yeung, K.W.K., Pan, H., Chu, P.K., Wu, S., 2017. Synergistic bacteria-killing through photodynamic and physical actions of graphene oxide/ag/collagen coating. ACS Appl. Mater. Interfaces 9 (31), 26417–26428.
Zakhidov, E.A., Zakhidova, M.A., Kokhkharov, A.M., Nematov, K., Nusretov, R.A., Kuvondikov, V.O., Saparbaev, A.A., 2017. Raman spectroscopy of the interface between a thin nanostructured ZnO film and fullerene C60. Opt. Spectrosc. 122 (4), 607–614.
Zhang, Y., Liu, X., Li, Z., Zhu, S., Yuan, X., Cui, Z., Yang, X., Chu, P.K., Wu, S., 2018. Nano Ag/ZnO-incorporated hydroxyapatite composite coatings: highly effective infection prevention and excellent osteointegration. ACS Appl. Mater. Interface 10 (1), 1266–1277.
Zhao, X., Lv, L., Pana, B., Zhanga, W., Zhanga, S., 2011. Polymer-supported Nano composites for environmental application: a review. Chem. Eng. J. 170, 381–394.